Book Section:
Peckham, M. (2024) Using high resolution imaging to investigate cell migration in vitro. In: Brüning-Richardson, A. and Knipp, S., (eds.) Cell Migration in Development, Health and Disease. Springer Cham, pp. 201-221. ISBN: 9783031645310.

https://doi.org/10.1007/978-3-031-64532-7_9

Using high resolution imaging to investigate cell migration in vitro

Michelle Peckham, School of Molecular and Cellular Biology, Faculty of Biological Sciences, University of Leeds, Leeds, LS2 9JT
m.peckham@leeds.ac.uk

Chapter Table of Contents

What you will learn in this chapter

A wide array of fluorescence microscopy approaches is used to image cultured cells in vitro. This type of approach is widely used for imaging the behaviour of specific proteins within cells to understand their dynamic behaviour and location. Within the last 20 years, multiple different forms of fluorescent microscopies have been developed to achieve this. With the vast array of different approaches available, it can be difficult to know where to start. This chapter provides a simple introduction to high resolution fluorescence microscopy approaches to image cells in vitro for beginners, how to choose the right approach and how to optimise your imaging.

Keywords:
Fluorescence microscopy, in vitro, cell culture, fluorescent proteins, structured illumination microscopy, light sheet microscopy, total internal reflection fluorescence microscopy,

1 Background to fluorescence microscopy: fluorescent proteins and super-resolution imaging

A widely used approach to locating proteins in cells is to express the cDNA for the protein fused to a fluorescent protein (FP) such as eGFP (enhanced green fluorescent protein) in cells and perform live cell imaging. A more sophisticated approach is to use CRISPR or a related approach to label the endogenous protein (Bukhari and Muller, 2019). This has the advantage that the fluorescently labelled protein of interest should be expressed at endogenous levels. However, this is a more challenging technique. In addition, small tags (Halo, SNAP) that can then be labelled with cell-permeable dyes and other approaches are used (Liu and Cui, 2020). Other forms of FPs are continually being developed (Cranfill et al., 2016), each with specific advantages and properties.

Transient expression of eGFP fused to the protein of interest is a straightforward way to initially assess if the fluorescently tagged protein localises correctly in live cells. Its localisation should be similar to that observed when using antibodies to determine the localisation of the protein of interest. It also enables the researcher to quickly test if fusing eGFP on the N- or C-terminus works best, or if one or the other can compromise the localisation of the protein. For example, α-actinin in which eGFP is fused to the C-terminus of localises correctly, but α-actinin in which eGFP is fused to the N-terminus does not (Dabiri et al., 1997). Although many FP variants have been described since GFP was first used as a reporter many years ago (Chalfie et al., 1994), it still performs really well, and we routinely use the enhanced version of GFP (eGFP; (Yang et al., 1996)) for initial assessments of FP fusions in cells.

While eGFP is useful for many experiments, we recommend using FPbase (Lambert, 2019), to choose suitable FPs for specific experiments, especially when combining multiple FPs. The excitation and emission spectra need to be carefully checked to make sure that users have the appropriate light sources (lasers) to excite the FP at the correct wavelength, and appropriate filters to image the emitted fluorescence. It is important to check the overlap of the emission spectra when using multiple fluorophores, to make sure they are well separated. FPbase is useful in being able to select the brightest

fluorophores, as it provides values for the theoretical brightness (linked to the quantum efficiency (QE) for each FP. However, it is always best to test specific FPs in your specific experimental system and compare them to eGFP. Finally, FPbase also indicates if a specific FP tends to dimerise, which typically should be avoided when using FPs to tag proteins of interest.

Resolution and Super-resolution: The resolution of a wide-field fluorescence microscope is approximately half the wavelength of the emitted light being imaged (e.g. ~250nm for a wavelength of exciting light of 488nm, the wavelength used to excite eGFP (Fig 1A,B)). What this means, practically, is that two fluorescent objects in an image that are less than 250nm apart, cannot be resolved as two separate objects in the final image, but will be observed as one single blurry fluorescent object. A wide range of novel microscopical approaches have been developed to overcome this problem with resolution and in some cases, FPs have played a role in developing some of these.

The main reason why wide-field light microscopes are limited to a resolution of ~250nm is due to diffraction (bending) of light as it passes through the sample and objective lens. Simply put, small objects diffract the light to wider angles than larger objects (Fig. 1C). The result is that a small point object in a sample is imaged as a blurry spot. In XY, this blurry spot is also referred to as the Airy disk (Fig. 1D). In XYZ, the blurry spot is also referred to as the point spread function. The size of the numerical aperture (NA) of the lens limits how large an angle of light it can collect from any object; the larger the NA, the greater the amount of light it can collect. However, the highest NA for most objective lenses is 1.4. (Incidentally, the image resolution for any lens with a NA of 1.4 is the same, even when one lens has a magnification of x 40 and the other of x 100). Diffraction also depends on the wavelength of the light, with longer wavelengths (towards the red end of the spectrum) diffracting light to a larger angle than shorter wavelengths, and on the refractive index of the imaging medium (e.g. oil immersion vs water or air immersion lenses). The physics behind image formation was solved in 1873 by Ernst Abbe. Using his equation ($d=\lambda/2$ N.A.), the best resolution is approximately half the wavelength of the light used to image the sample. This effectively means that two objects closer than ~250nm cannot be resolved as two separate spots (Fig. 1D). Incidentally, this is the resolution in XY (lateral). Resolution in Z (axial) is almost 3 times lower.

The easiest and probably most accessible approach for super-resolution imaging is to use an enhanced form of microscopy provided on some Zeiss confocal microscopes, called 'Airyscan'. Confocal microscopy uses a point source of light (laser scanning) to excite the sample, and the emitted fluorescent light has to pass through a pinhole before it is detected. This approach rejects the out of focus fluorescence resulting in sharper images. However, it also results in a small increase in lateral resolution (Wilson, 2011). Reducing the size of the pinhole would increase this resolution further, but the resulting image would be very dim, as most of the light would be rejected by the pinhole, and not be recorded on the detector. Airyscan overcomes this by using a 32-element array, in which each element has an effective pinhole of 0.2. The 32 images recorded by each element are combined and processed to generate a final image with ~1.7fold increase in lateral resolution, and near normal intensity. As this is commercial solution, commonly included with a confocal system, this approach is widely available, and straightforward to implement. Moreover, it works with all standard dyes and fluorophores, as used in standard widefield or confocal imaging, as illustrated here for tubulin (Fig. 1E,F).

An alternative approach to Airyscan, with similar improvement in resolution is structured illumination (SIM). Many imaging facilities are now equipped with some sort of SIM microscope. In simple terms, SIM uses a fine pattern of light to illuminate the sample (Gustafsson, 2000). This interacts with the fine pattern within the sample itself (of a similar frequency) generating an interference pattern that effectively reduces the spread of the diffracted light by half, thus doubling resolution. To be able to arithmetically separate the real image from the pattern, typically, 9 images need to be obtained, in which the pattern is rotated between each one. These images are then processed via Fourier transformation and then back into real space to generate an image of the original sample at twice the resolution. The original SIM microscope used a physical grating, but new and commercial versions now use spatial light modulators that generate patterns more quickly. This approach has been further developed to generate a lattice pattern rather than stripes in the Zeiss Elyra SIM and a newer implementation (SIM^2).

Our laboratory has an iSIM microscope, which works in a slightly different way (Curd et al., 2015; York et al., 2013). The sample is illuminated by a pattern of light that is generated by a lens array, in

which a laser is rapidly scanned over each of the multiple lenses simultaneously. The emitted light passes through a pinhole array, and then through a second lens array that contracts each spot by x2 before being detected by a scientific CMOS camera. The final obtainable resolution (after a subsequent deconvolution step) is ~ x2 fold, similar to that of Airyscan. A commercial version of this microscope has also been developed (Visitek). The key advantage of this approach is that the improvement in resolution is achieved through the optical design, and thus it does not require any image processing. Further advances for iSIM have included improved deconvolution using machine learning approaches (Guo et al., 2020).

Two further main types of super-resolution include STED (stimulated emission depletion microscopy; (Hell and Wichmann, 1994; Klar and Hell, 1999)) and single molecule localisation microscopies (SMLM). In simple terms, STED is a modified form of confocal microscopy. In addition to illuminating the sample with a scanning point source of light, a second 'depletion' laser, which is donut shaped is also scanned over the sample at the same time. This switches off the fluorescence of the fluorophores within the donut, effectively shrinking the size of the spot that can emit fluorescence. The improvement in resolution depends on the square root of the intensity of the depletion laser, which can be varied. Typically, this is around 50nm in XY, on a commercial microscope (STEDYCON, supplied by Abberior). This resolution improvement is entirely optical, and does not require any image processing, but the final images do benefit from deconvolution. However, unless the microscope also has a depletion laser for the axial direction, resolution in Z is no better than confocal. In addition, as this approach depends on the interaction of the depletion laser with the dye, specific dyes need to be used for the best performance in STED (see https://abberior.rocks/dyes-labels/) and eGFP constructs do not work very well. In the example shown here (Fig. 1E,F), a 'star-red' dye was used. More typically, constructs with Halo-Tags are used, with specific STED dyes designed for live cell imaging using STED (https://abberior.rocks/dyes-labels/abberior-live/).

Single molecule localisation microscopies include PALM (photoactivatable light microscopy) and dSTORM (direct Stochastic Optical Reconstruction Microscopy). These techniques can provide a resolution of ~ 20nm. PALM was first demonstrated using photoactivatable GFP (paGFP; (Betzig et al., 2006)). paGFP is not fluorescent until it is excited by short wavelength (405nm) light. By controlling the levels of illumination, only a small subset of molecules become fluorescent at any one time, and these tend to be well separated spatially (e.g. separated by more than 250nm). Thus, these molecules can be resolved, and the position of each molecule identified accurately. Eventually, the molecules bleach, and small numbers of new fluorescent molecules appear. By imaging small numbers of fluorescent molecules that appear randomly from frame to frame, over many, many frames (~5000-10000), the positions of all the molecules are then identified and used to reconstruct the final image.

For PALM to work well, the rate at which the FP interconverts between the dark and fluorescent states must be low compared to the rate of conversion initiated by light activation. In addition, the fluorescence of the dark (inactive) FP must be low compared to that of the active (fluorescent) molecule, a property known as the contrast ratio (Hess et al., 2006). paGFP turns out not to be the best FP for PALM as it has a relatively low contrast ratio, while that for pamCherry is 400x better (Allen et al., 2013). The drawback of both these FPs is that transiently transfected cells are not fluorescent, and thus cannot be identified until they are illuminated with 405nm wavelength of light.

Currently, the most commonly used FP used in PALM is derived from EosFP (McKinney et al., 2009; Wiedenmann et al., 2004). EosFP is a type of fluorophore that photoconverts from a green to a red fluorescent state, when illuminated with 405nm wavelength of light, and it has a high contrast ratio (Allen et al., 2013). Transfected cells can thus be identified before imaging them using PALM, as they fluoresce when excited with 488nm wavelength light. EosFP has since been engineered to be monomeric (Zhang et al., 2012) and mEos3.2 is now commonly used. mEosFP is also useful in analysing protein dynamics, in a technique analogous to FRAP (fluorescence recovery after photobleaching). For example, we have used this FP to analyse the turnover of α-actinin-2 (ACTN2) in the Z-discs of cardiomyocytes (Haywood et al., 2016).

STORM, originally developed by Xiowei Zhuang at about the same time as PALM (Rust et al., 2006), used antibodies labelled with two fluorescent dyes, in which one of the two dyes is bleached, a small number of the bleached molecules is switched back on by exciting the second dye, these are well separated spatially, and their positions accurately identified. It was later discovered that adding β-mercaptoethanol (which encourages some dyes to enter a dark 'triplet' state) and oxygen scavengers

(which slow the re-formation of the ground state) to the imaging buffer, keeps most of the dye molecules in a dark state. A small number of dye molecules can then re-enter the ground state when illuminated with short wavelength light (405nm) and can then be excited and fluoresce following illumination with the appropriate wavelength of light for that dye, and positions identified accurately (Heilemann et al., 2009; Heilemann et al., 2008). This approach is known as dSTORM (directSTORM) and is the most commonly used approach for SMLM based super-resolution for fixed cells. However, the best dye for dSTORM is Alexa 647 (as shown in the example here: Fig 1E,F) (Dempsey et al., 2011).

All of the SMLM techniques are challenging to use in live cell imaging as they all require several thousand frames to be collected to reconstruct the final image. Using antibodies for visualising proteins within living cells is clearly challenging, as it relies on a good method to deliver the labelled antibodies, and a benign effect of the antibodies once inside the cells. Moreover, the challenge is to be able to track single fluorophores, and yet for the fluorophores to be well enough spatially separated to reconstruct a final image at high resolution. However, photoactivatable or switchable fluorescent proteins have been used in live cell imaging, a technique named sptPALM. sptPALM was first described using Eos-FP tagged molecules, in which small subsets of molecules were switched from green to red fluorescence, and the red fluorescent molecules were tracked and their positions identified (Manley et al., 2008). However, this does require illuminating cells with 405nm wavelength light, to induce the switch from green to red, which tends to be more cytotoxic for cells than longer wavelengths of light. Despite this, sptPALM is likely to become more popular in the future, with improvements in illumination technologies, and the greater need for imaging in live cells.

Finally, while not strictly a super-resolution imaging approach, light sheet imaging, and specifically lattice light sheet imaging is starting to become more widely used. In widefield, confocal and super-resolution imaging, only a single XY plane is imaged at any one time, but the entire sample in the field of view is illuminated. Fluorophores above and below the plane of imaging are also excited and fluoresce but are not imaged. This can lead to photobleaching and phototoxicity, which ideally should be avoided in live cell imaging. In light sheet (selective plane illumination) microscopy, the sample is illuminated by a thin sheet of light, which is the same as the plane that is being imaged (focal plane) (Huisken et al., 2004). Fluorophores outside this plane of light are not excited, thus, there is no out of focus fluorescence, which improves axial resolution, and photobleaching and toxicity effects are reduced.

There are many forms of light sheet microscopes, and these mostly differ in the width of the light sheet that they are able to generate. Ideally, the width of the light sheet should be much narrower than the sample being imaged. Moreover, the lateral width of the light sheet also determines the axial resolution. Lattice light sheet (LLS) generates an ultrathin light sheet that is suited to imaging single cells, spheroids, small organoids and small organisms such as *Drosophila* embryos (Chen et al., 2014). The lattice light sheet uses a specific form of illumination to generate a narrow light sheet, down to ~500nm in width (and 12 μm long), much smaller than the dimensions of a single cell (around 20-50μm in width). In LLS, the light sheet is rapidly scanned across the cell (or field of view) to generate the image and an entire cell volume can be scanned in less than a second. The resolution obtainable is about 290nm in XY and as little as 450 nm in Z, and thus the resolution is XY is more similar to that in Z compared to confocal. The original version of LLS uses dipping lens and an upright microscope configuration (objective is above the sample), to avoid optical aberrations introduced due to a change in refractive index between water and glass. A commercial version of LLS developed by Zeiss is now available, which uses an inverted configuration, and overcomes the optical aberrations through the use of an Alvarez plate. Experimentally, light sheet is also being developed for imaging single molecules in living cells (Ponjavic et al., 2018).

Overall, there is a wide array of different imaging approaches to choose from. Which microscope you do eventually choose is going to depend on if it is easily available, if it is equipped for live cell imaging, and if it is able to image at the resolution and speeds that you need for your samples. Typically, these advanced microscopes are found in facilities and looked after by well-trained staff who can advise and help you with your imaging. For more broader reading, two recent reviews summarise a variety of super-resolution and other imaging approaches in more detail (Jacquemet et al., 2020; Schermelleh et al., 2019) and can help you to decide which type of imaging you need for your specific experiments.

2 Preparation and transfection of cells for live cell fluorescent imaging

Most cultured cells can be used in live cell fluorescent imaging, for example using eGFP-tagged proteins. To test out a new eGFP-tagged protein, we typically use a transient transfection method, and easy-to-transfect cultured cell lines (e.g. HEK-293 (Human embryonic kidney 293) or COS-7 (African green monkey kidney fibroblast-like)). However, while easy to transfect, the cytoskeleton and general morphology of these cells can appear less well-developed than other cell lines, and we find they can be less suited for specific experiments designed to interrogate cell migration and the cytoskeleton. Therefore, we choose other cell types depending on the experiment we want to undertake. For example, B-16-f10 cells (a mouse melanoma cell line) are useful for research into actin dynamics in the lamellipodium (Lopata et al., 2018), muscle myoblasts key for research into myoblast fusion (Swailes et al., 2006; Swailes et al., 2004) and PC-3 (human prostate cancer) cells are useful for investigations into how myosin isoforms specifically affect cytoskeletal organisation and cell migration (Makowska et al., 2015). All of these cell lines and many others are available from ATCC (American Tissue Type Collection).

DNA: We occasionally use DNA expression plasmids purified by miniprep for a quick test, but transfection rates are lower. More routinely, we use maxiprepped DNA, purified using a Qiagen Plasmid kit, following the manufacturer's instructions. The purified DNA is sterile as a result of the ethanol or isopropanol final washes. We measure the concentration using a nanodrop at a wavelength of 260 nm. Measuring the 260/280 ratio can be helpful in checking purity. We store the purified DNA in sterile TE (Tris-EDTA) or distilled water at -20°C, aiming for a final concentration of ~1mg/ml.

Glass culture surfaces and methods for cleaning: For live cell imaging, we typically use glass-bottomed dishes. Plastic-bottomed dishes are highly autofluorescent, are poor optically and should be avoided. Typically, we use glass bottomed dishes from IBIDI (Cat.No:81218-200) or equivalent, which have a #1.5 glass coverslip on the bottom of the dish (170 μm thick). This thickness is important for obtaining the best images, as most microscope objectives are optimised for this thickness. We occasionally use glass bottomed multiwell dishes as an alternative. The dishes may need pretreating to enable the cells to stick to the surface with poly-L-lysine, laminin or other attachment factor. This needs to be tested for each cell type used.
Alternatively, for fixing and staining transfected cells, we use #1.5 glass coverslips, either 13mm in diameter, or square (20 x 20 mm). These complimentary experiments on fixed cells help us interpret protein localisation in live cells. In this case, it is critical to make sure that the coverslips are washed first. Coverslips straight out of the box are dusty, dust is fluorescent and will impact on image quality. (Sterile glass bottomed dishes are usually clean enough to use straight away). There are many different ways that the coverslips can be washed. The simplest is to wash them in hot water with a small amount of liquid detergent (washing up liquid). We put the whole pack (~100 coverslips) into a 50ml falcon tube filled with hot water and a small squirt of detergent, continuously invert the tube for 1-2 minutes, pour away the detergent mix, wash x 5 (5 complete changes) in hot water, then x 5 in cold water, x 5 in distilled water, and then store the coverslips in 70% ethanol. Alternatively, the coverslips can be washed in a similar way, using 1M HCL instead of detergent, followed by x10 washes in distilled water (complete volume changes) before storing in 70% ethanol.
For more challenging super-resolution applications, specifically dSTORM of fixed cells, we use an extensive acid wash. We use #1.5 glass square (20 x 20mm) coverslips, which we place in a coverslip minirack (e.g. C-14784 from Thermofisher: acid resistant). We wear gloves to prevent contact of the caustic chemicals used with the skin. In the fume hood, we first combine 125ml distilled water, 25ml ammonium hydroxide and 25ml hydrogen peroxide, measured out using a 100 ml measuring cylinder, in a 250 ml glass beaker. The beaker is then placed on a hot stirrer set to 80 °C, with a stirrer in the bottom. The coverslips in their rack are placed into the beaker such that the coverslips are submerged and left in the cleaning solution for at least 3 hours, while stirring. At the end of this incubation period, the rack and coverslips are transferred into a fresh 250 ml beaker with at least 150ml of clean distilled water, and then washed a further 9 times, with fresh 150ml of distilled water each time. The rack is then transferred into a beaker of methanol, or 70% ethanol. At this point, single coverslips can be removed

using tweezers, and sterilised by briefly passing the coverslip through the tip of a Bunsen flame, before placing into a clean dry staining rack, in a suitable container. Once this is done for all the coverslips, they can be covered and stored dry. However, care is needed here as it is very easy for the coverslips to crack in the heat. Cells are grown on these coverslips, pre-coated with attachment factors as necessary. They are then fixed, stained, and inverted onto microscope slides with a single glass cavity which we fill with dSTORM imaging buffer and seal, ready for imaging.

Transfection of cells: The day before transfection, the cells are passaged, and plated out at the required cell density on imaging dishes or coverslips, coated as required if necessary. To do this, first the growth medium is removed from the cells, and sufficient TrypLE to cover the growing surface (e.g. ~1ml for a 25cm^2 flask) is added, the flask is placed back in the incubator (37°C) for 1-2 mins, then observed using a phase contrast microscope (Nikon, inverted, x10 objective) to check for cell detachment. Next, fresh growth medium (e.g. DMEM, 10% serum, pen/strep, for HEK293 cells: 10mL for a 25cm^2 flask) is added to the flask to inactivate the TrypLE, the medium containing the detached cells is removed, added to a 15mL sterile falcon tube, and centrifuged for 5 minutes at 1000rpm to pellet the cells. Almost all of the growth medium is aspirated, the cell pellet is loosened by gently flicking the bottom of the tube and then resuspended in 1ml of growth medium. A small (~10µl) aliquot of cell suspension is removed and used to count the cell density using a Neubauer haemocytometer. The cell concentration is adjusted to ~ 5 x 10^5 cells per ml, by adding additional growth medium as required. 400 µL (~20,000 cells) is added to the glass dish, which has a growth area of 3.14 cm^2. This results in ~60,000 cells per cm^2 (or 1 x 10^6 µm^2), ~50-80% confluent. The cells are allowed to attach for 5-10 minutes, then further growth medium is added to a final volume of ~2ml. Alternatively, we add the cells in small 50 µl drops across the dish, allow the cells to attach for 5-10 minutes, and then add 2ml of growth medium. This can be a useful way to obtain a variable cell density across the dish,
To transfect the cells, we typically use Fugene 6, but there are many alternatives, and we do occasionally use nucleofection (electroporation). Ideally, different transfection methods should be tested for each new cell line. All of the following steps are performed in a tissue culture hood under sterile conditions. FuGENE 6 is stored in the fridge, until use, and then allowed to come up to room temperature for about 15 minutes prior to transfection. We normally use 3:1 of reagent to DNA (6µl fugene, 2µg DNA). Briefly, 6 µl of FuGENE 6 is directly pipetted into ~92 µl serum free medium (DMEM, without antibiotics) in a 1.5ml sterile Eppendorf tube and mixed by flicking the tube briefly. The mixture is incubated for 5 minutes, and then 2 µg of DNA plasmid (in 2 µl) is added, such that the final volume is 100 µl (initial volume of DMEM needs to be adjusted for volume of DNA to be added). The solution is mixed by briefly flicking the tube and left to incubate for a minimum of 15 minutes at room temperature. This mixture is then added dropwise to the cells, and the dish placed back in the incubator. The cells are then ready to image 24-48 hours later.

In addition to transfection, there are many small molecule fluorescent probes that can be used in imaging, which can just be added to live cells and then the cells can be imaged after a short incubation period (~1 hour). We have used SPY-DNA, SPY-F-actin (fluorescent latrunculin,) and SPY-tubulin (fluorescent taxol) (Lukinavicius et al., 2014). These are now all commercially available from Spirochrome.com and all seem to work reasonably well. There are also fluorescent probes for organelles such as mitochondria (Mito-Dye (Biotium) and MitoTracker (Thermofisher) and lysosomes as well as membrane mitochondrial and endoplasmic reticulum membrane tension reporters (also commercially available from Spirochrome). As with everything, these should all be tested in your system to see how well they work for you. Companies are usually willing to provide test samples for free, to allow you to do this.

Spheroids: Occasionally, we make small spheroids using transfected cells. We typically use permanently transfected cells, but transiently transfected cells can also be used. To generate permanently transfected cells, the method of transfection is the same as described above, but the cells are plated into a well of a 6 well culture plate for transfection. The day after transfection, we passage the cells into a fresh well and add fresh growth medium supplemented with G418 (geneticin: an aminoglycoside antibiotic). The majority of eGFP (or other) expression plasmids contain a resistance gene that allows cells to survive in the presence of G418. We determine the concentration of G418

required for each cell line beforehand, such that >90% of untransfected cells are dead within 5 days. After 7-10 days of selection, the cells can be kept as a mixed line of eGFP-construct expressing cells, or fluorescent cells can be isolated by FACS (flow assisted cytometric sorting), plated out at ~1 cell per well in a 96 well dish and allowed to grow up to obtain unique clones. Alternatively, at the point of first adding G418, the cells can be counted and plated at low density (~1 x 10^4 cells per ml in 20mL, on a 25cm^2 dish) for clonal selection, and then individual clones selected 7-10 days later.
To make spheroids, we use two main approaches. In the first, we use non-adherent dishes (e.g. Nuclon Sphera multiwell dish). Cells are trypsinised and counted as before, and diluted to 5x 10^3 cells/ml. The appropriate volume is then added to each well of the non-adherent plate (e.g. 200 µL for a 96 well, 500 µL for a 24 well plate and so on). Spheroids are ready to image about 3-4 days later. Alternatively, we use a simple hanging drop approach. About 10ml of sterile PBS is added to the bottom of a 100mm diameter plastic culture dish, cells are diluted to ~1-2 x 10^3 cells/ml and multiple drops (50 µL each) of the cell suspension (~800 cells) are pipetted onto the upturned lid, such that the drops are well spaced. The lid is then carefully inverted and placed on top of the culture dish. The cells form spheroids within ~ 2 days.

4. Preparation and transfection of cells for live cell imaging

24-48 hours after transfection, we inspect the cells on a widefield inverted fluorescent microscope to check that a reasonable number (>20%) of cells are expressing the eGFP (or other FP) construct of choice. We then routinely add 10-20mM sterile HEPES buffer (from a 1M stock) to the medium prior to imaging. We do this as most cell media contain sodium bicarbonate, which is both required for healthy cell growth, and provides pH buffering in combination with the CO_2 in the incubator to maintain the correct pH. However, depending on the microscope available, it is not always possible to maintain a 5% CO_2 environment. HEPES works reasonably well for a few hours to maintain pH instead.

Using the standard growth medium for live cell imaging is good for cell health, but standard medium contains phenol-red (as a pH indicator) and serum, which are both fluorescent. If the eGFP signal is weak, then we have used commercial imaging solutions that are phenol-red and serum free. These include Live cell imaging solution (Fisher scientific) and Fluorobrite DMEM (Thermofisher Scientific). Live cell imaging solution contains 140mM NaCl, 2.5mM KCl, 1.8mM $CaCl_2$, 1.0mM $MgCl_2$ and 20mM HEPES, but does not contain glucose or serum, and thus is only suitable for short (up to ~4 hours) of live cell imaging. Fluorobrite is effectively phenol-red free DMEM and will support longer term culture when supplemented with serum and glutamine (or glutamax), and additionally needs the addition of HEPES for non-CO_2 environments.

To image spheroids, we use low melting point agarose (suitable for cell culture, e.g. from Sigma Aldrich) to immobilise them. We make up a 1% solution (0.5g of agarose is added to 50mL of water in a sterile 50mL Falcon tube), heat this in a microwave until the agarose dissolves, and cool to ~40°C in a water bath or equivalent. A single spheroid is then carefully transferred from suspension culture (drops or plates), into 1 well of an 8 well glass bottomed dish in ~100µl of growth medium, supplemented with HEPES as required, 100 – 200 µl of the warm agarose is added, and the dish transferred back to the incubator. The ratio of agarose to growth medium will determine how 'solid' the final gel is once the agarose has set. We do not use Matrigel for imaging, as it scatters too much light, which degrades image quality.

5. Confocal and Airyscan imaging

We routinely use a Zeiss LSM 880 confocal equipped with fast Airyscan for live cell imaging, using the x40 N.A. 1.4 oil immersion objective. The microscope is equipped with a heated stage, which we switch on and allow to heat up to 37 °C for 30-60 minutes before imaging. This helps to avoid thermal

drift, and thus samples going out of focus, once imaging starts. The sample is placed on the stage, and first examined using the eyepieces, before switching to confocal mode. Even if the plan is to use Airyscan, we normally take an initial image using the confocal mode, exciting eGFP with the 488 nm wavelength laser, Airy set to 1, and adjusting laser intensity and gain to obtain an initial image with good signal to noise (high signal from the eGFP, low noise from the background). We then switch to Airyscan, select the SR (super-resolution mode) and again adjust laser intensity and gain as required. We then select the start and end points in z to collect a z-stack. If we initially need to characterise protein organisation throughout the entire depth of the entire cell, then we will collect a z-stack from the top to the bottom of the entire cell (Fig. 2A). This helps us determine where, in z, we wish to collect further data, and which region of the cell we might want to crop into (e.g the leading edge of the cell, etc). Subsequently, we will use a single plane or short z-stack, for a small region of interest (Fig. 2B).

Selecting the size and position of the z-stack and the timing interval is sample dependent in live cell imaging. The first time we image any new construct we will test out different sizes of z-stack and timing intervals. For fast moving objects within the sample, we need to image at the highest frame rate possible. In some cases, we can predict this beforehand. For example, kinesin moves along microtubules at a speed of ~ 0.5-1 μm per second. To be able to reliably track single fluorescent kinesin spots from frame to frame, using a microscope with a resolution of ~0.3 μm, we can calculate that we need a minimum frame rate of 2 frames per second to be able to accurately identify the same spot from frame to frame and measure the speed at which it moved (Dunn et al., 2008). In other cases, without prior knowledge, we try different frame rates to determine which one works best for the behaviour we wish to quantify.

For example, we can use the Airyscan to image a large Z-stack of a cell expressing the eGFP-tagged protein of interest, such as eGFP-tagged Myo1E (Figure 2). Although the Z-stack of almost the entire cell provides a good overview of its morphology and indicates that eGFP-Myo1E is mostly located in the cellular cortex and in filopodial structures, imaging the entire Z-stack over the entire cell for a time-lapse sequence, would be slow (about 1 Z-stack per minute), would not capture fast events, and is likely to be phototoxic. However, the Z-stack does show that many filopodia are located towards the basal region of the cell, and at the cell periphery, enabling us to make a reasonable judgement about where it is most important to image if we need to quantify the behaviour of the filopodia, for example.

For this example, we chose to reduce the size of the Z-stack to 3.29 μm (19 x 0.173 μm steps), and we cropped in on a smaller region near the edge of the cell that is rich in protrusions (XY:444 (18.9 μm) x 444 pixels) by increasing the zoom to x10.9). This enabled us to capture a Z-stack at a much faster rate (One Z-stack in <1 second). This is still relatively slow, and if speed were an issue, we could crop into a smaller region, and reduce the Z-stack still further, to a single frame if necessary, and/or reduce the resolution of the image. The key decision is how fast do we need to image, and can we just image a small region of the cell, to quantify the behaviour we are interested in. Here, the image capture rate is fast enough to observe the overall behaviour of the eGFP-Myo1E filopodia (growing, shrinking, overall numbers). However, if we needed to measure the dynamic movement of eGFP-Myo1E within the filopodia, we would likely need to increase the imaging rate by >5 times.

The Airyscan can be too slow for imaging rapid events, especially when a larger field of view is needed. In this case, we have switched to iSIM to image rapidly moving objects such as cytoplasmic granules containing virus protein in live cells (Remenyi et al., 2018). The iSIM can capture images at up to 100 frames per second for larger fields of view (90 μm x 80 μm (1745 x 1550 pixels) and the minimum Z-step size is 0.05 μm. To capture a Z-stack of 3.29 μm using a similar size of Z-step (0.173 μm) is thus 5 x faster than using the Airyscan, but with a much larger field of view. Scanning over a smaller error enables faster image capture rates. The final resolution of iSIM is similar to that obtained by Airyscan. However, the homebuilt iSIM is only equipped with two lasers (488nm and 561nm), and the rate of photobleaching on the iSIM is faster than it is on the Airyscan. Thus, this microscope is best for high resolution imaging over short time periods, and specifically for rapidly moving objects.

Finally, as more and more experiments are starting to use 3D cellular models such as spheroids and organoids, we have also used confocal imaging to image these types of samples. However, here we are

more interested in imaging several cells in the spheroid at once, and using a relatively fast frame rate, such that we can assess dynamic behaviour in a small region of the spheroid, and in this case, we imaged in a single plane only. This type of imaging is possible using the confocal and does show differences between different types of knockdown cells (Fig. 4). However, it would be more challenging to image larger Z-stacks at speed using this approach, while avoiding toxicity.

Lattice light sheet

An alternative approach for gentle imaging of a large volume of cells, or 3D imaging, is to use the lattice light sheet microscope. The sample preparation for this is exactly the same as for live cell imaging on the confocal, and glass bottomed dishes (#1.5) are required. The lattice light sheet is equipped with three lasers for excitation at 488nm, 561nm and 640nm (Imaging in the 'blue' range is usually more photodamaging for cells). It uses a water immersion lens for imaging (48 x, NA of 1.0). We typically use the 1000nm x 30 µm light sheet for imaging cells, spheroids and small organoids.

In lattice light sheet, the light sheet is scanned across the sample at an angle (Chen et al., 2014) at a rapid rate at intervals of 0.2µm (e.g. an image consisting of 10 planes would cover 2 µm). As with any microscopy, the speed of imaging the sample depends on how large a field of view you need to image, and this is adjustable in the software. However, a single time point (complete scan) using the 1000nm x 30 µm light sheet across a large field of view (Figure 5) that encompasses multiple cells in a small spheroid only took 4s. Cropping and imaging a smaller ROI would increase the image rate markedly. However, in this case, the larger field of view enables us to rapidly image many cells together in 3D, and visualise their interactions with each other (e.g. Fig. 5C, arrows).

Processing and Analysis

Finally, images are data. As with any data, they need to be processed and analysed. To process the data, we commonly deconvolve all the Airyscan and STED images of fixed cells, to provide a small (~1.4 fold) increase in resolution. We use Huygens Professional software or the Zeiss confocal software (Zen Blue) to do this. We do not usually do this for live cell images but do choose to do so if we need to see fine detail more easily. LLS images can also be deconvolved, and this needs to be done before deskewing (and the ability to do this is included in the Zen Blue software).
We analyse images in numerous ways, depending on what we want to quantify. We either use commercial software (Arrivis, Imaris, Huygens) to do this, or FiJi (Image J bundle). The ImageJ/Fiji website provides a downloadable version of ImageJ (https://imagej.net/software/fiji/). It is open source software (Schindelin et al., 2012) and many people do generate and upload useful plugins for the software that you can find here (https://imagej.net/plugins/). We have also developed our own software (e.g. an ImageJ plugin to analyse spheroids (Ketchen et al., 2020). ICY also provides free useful software for analysing images and this integrates with both ImageJ and Matlab (https://icy.bioimageanalysis.org/). In addition, we sometimes use Cell Profiler (https://cellprofiler.org/), now in version 4 (Stirling et al., 2021). All of these are worth trying to find the analysis best suited for your specific question. If you like coding (especially using Python) and need to develop segmentation of objects such as nuclei, organelles and cell bodies, then there is also Napari (https://napari.org/stable/) and Cellpose (https://cellpose.readthedocs.io/en/latest/index.html) (Stringer et al., 2021). We have also written Python based software to analyse patterns in super-resolution images (Curd et al., 2021).

Take Home Message starts

- Live cell imaging is important to understand the dynamics of cell behaviour, how the cytoskeleton reorganises with time, how organelles move around and so on.
- Many new approaches to live cell imaging have been developed over the past few years, and the resolution of the resultant images is improving.

- Super-resolution imaging techniques are challenging to apply to live cell imaging, but Airyscan, SIM (or iSIM) and light sheet are relatively straightforward to use.
- You should think of images as the 'data' and make sure you design your experiments appropriately, so that you can analyse what you need (e.g. choose the appropriate resolution, imaging speed, and region of interest that you need to answer your question and choose the appropriate image analysis that will help you analyse and quantify your data).

Take Home Message ends

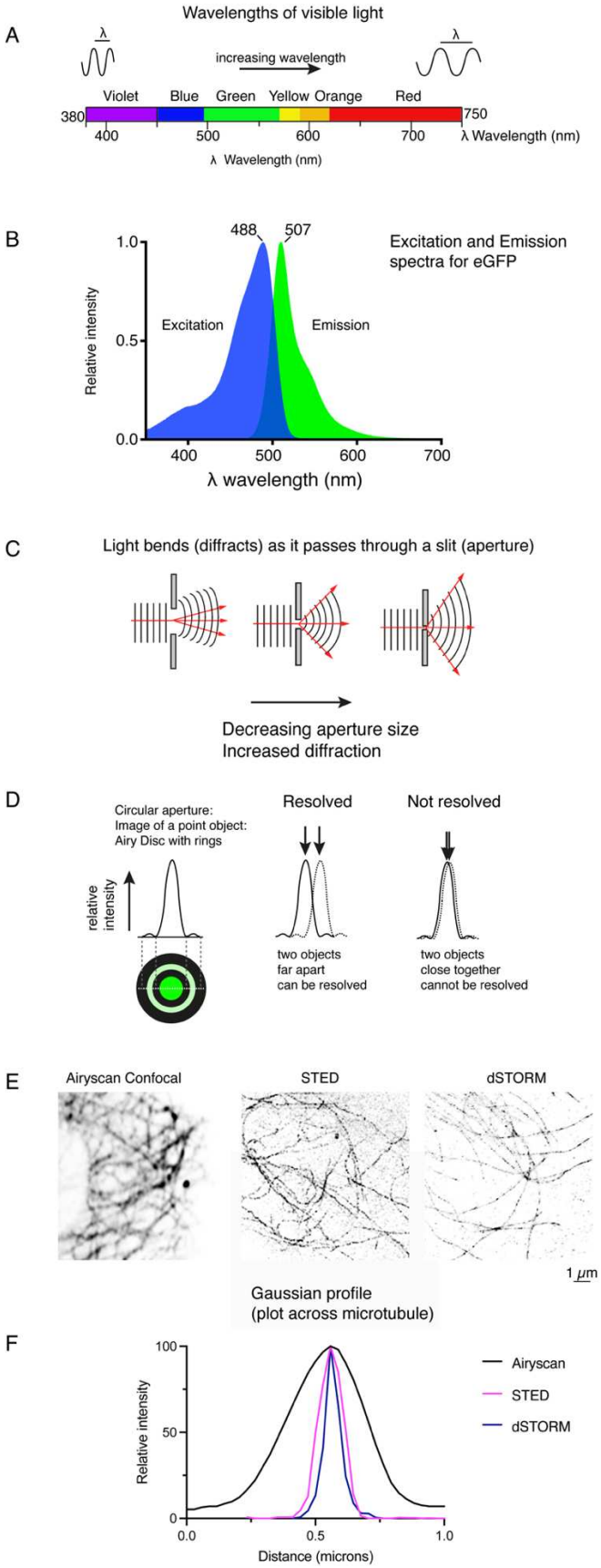

Figure 1: Resolution and super-resolution. A: wavelengths of visible light from short (~350nm) to long (~750nm). B: The wavelengths of light used to excite eGFP (blue: peak at 488nm) and the light emitted from excited eGFP (green: peak at 507nm). C: as light waves pass through a slit they bend

(diffract). The narrower the slit, the more they diffract. D. In microscopes apertures are circular rather than slits. The appearance of the final diffracted spot of light is shown (Airy disc), with its Gaussian profile (from line drawn across the centre of the disc). When two spots are far apart, the two spots are resolvable, but when they are close together they are not (as illustrated here by the two profiles for each spot). E. Example images from Airyscan confocal, STED and dSTORM of tubulin in microtubules, labelled using an antibody and an appropriate fluorophore (on the secondary antibody), together with an example profile for a region of microtubule using each of the three techniques. The improved resolution is linked to the narrower profile.

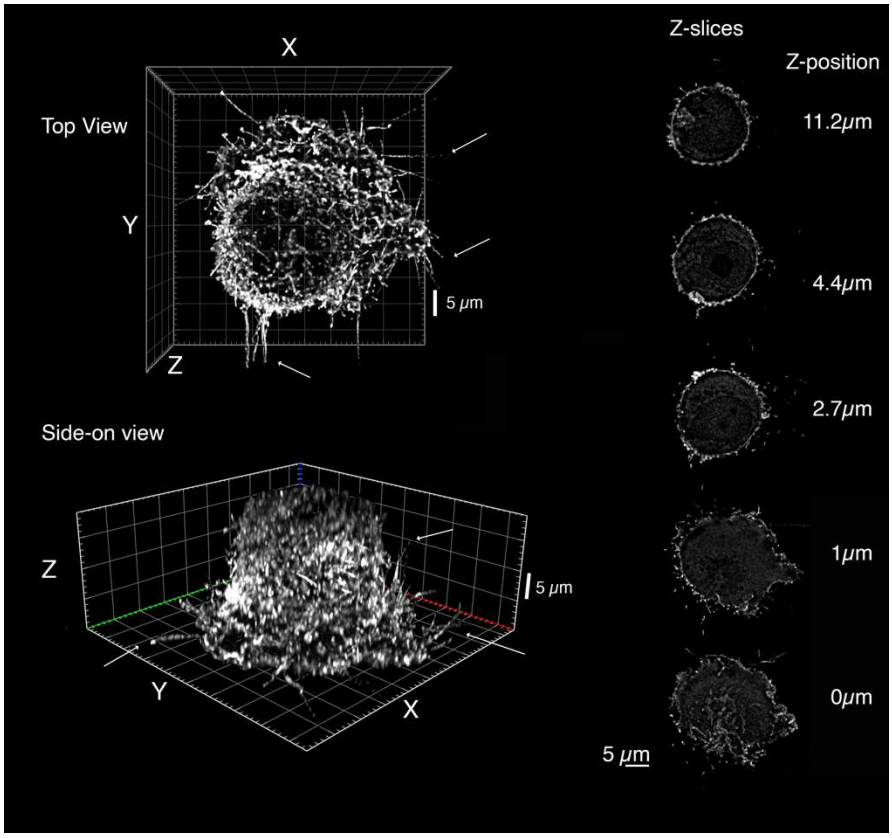

Figure 2: Airyscan Imaging of a live PC3-cell expressing eGFP-Myo1E. A Z-stack (900 (38.32 µm) x 900 pixels in XY and 88 slices (steps) 0.173 µm apart: 15.22 µm in Z) using a zoom of 5.5, took 52 seconds. A top view (all the individual images in Z projected into a single image, looking down from the top) and a side on-view shows the overall shape of the cell. eGFP-Myo1E positive filopodia (arrowed) are observed. Individual slices are shown on the right-hand side at different depths from the basal region of the cell (0 µm) towards the top (11.2 µm)

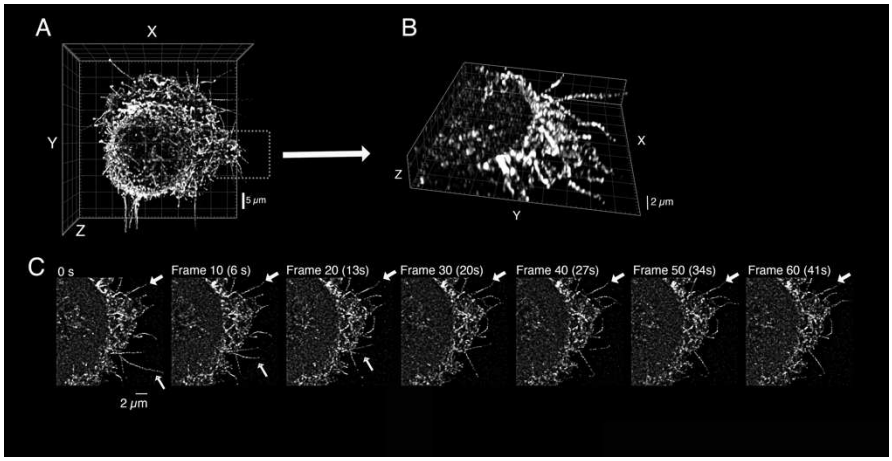

Figure 3: Fast Airyscan imaging of a region of interest (ROI) for a PC3-cell expressing eGFP-Myo1E. From the original Z-stack of the whole cell, we chose a ROI (indicated by the dashed square in A) and imaged this (ROI: dimensions are 18.9 x 18.9 x 3.29 μm: XYZ). B. shows a side-view projection image of the first frame. C. Shows individual maximum intensity projections (MIPs: all the images are combined into a single image, based on maximum intensity) for selected time points. Thick arrow indicates a filopodium that remains through most of the images. Thinner arrow (below) indicates a shrinking filopodium, only present up to frame 20 (13s).

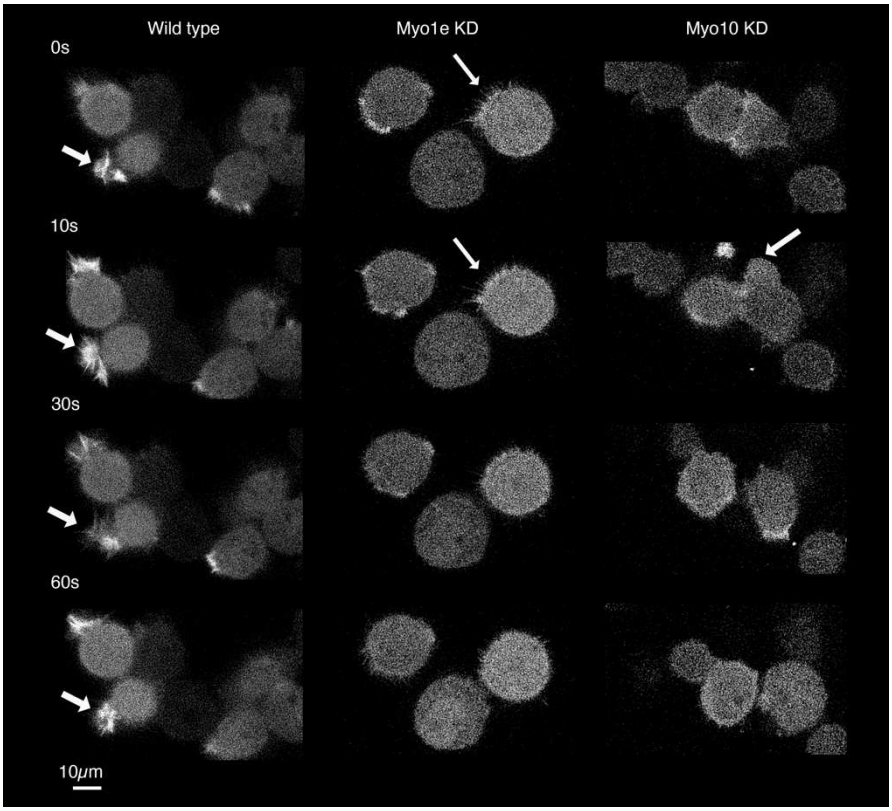

Figure 4: Confocal imaging of PC3-cell spheroids, expressing eGFP-lifeact. eGFP-lifeact labels F-actin in cells (Riedl et al., 2008). A single plane, and selected time points from 0 to 60s are shown. The images compared wild type PC3 cells, with those in which Myo1e of Myo10 have been knocked down (KD) using siRNA. The lack of well-focussed, eGFP-lifeact rich (and thus actin rich – arrowed for wild type) protrusions are evident in both types of knockdown cells. In Myo1e KD cells, fine protrusions are still present (arrowed), but in Myo10 KD cells, the cells only seem competent to form blebs (arrowed).

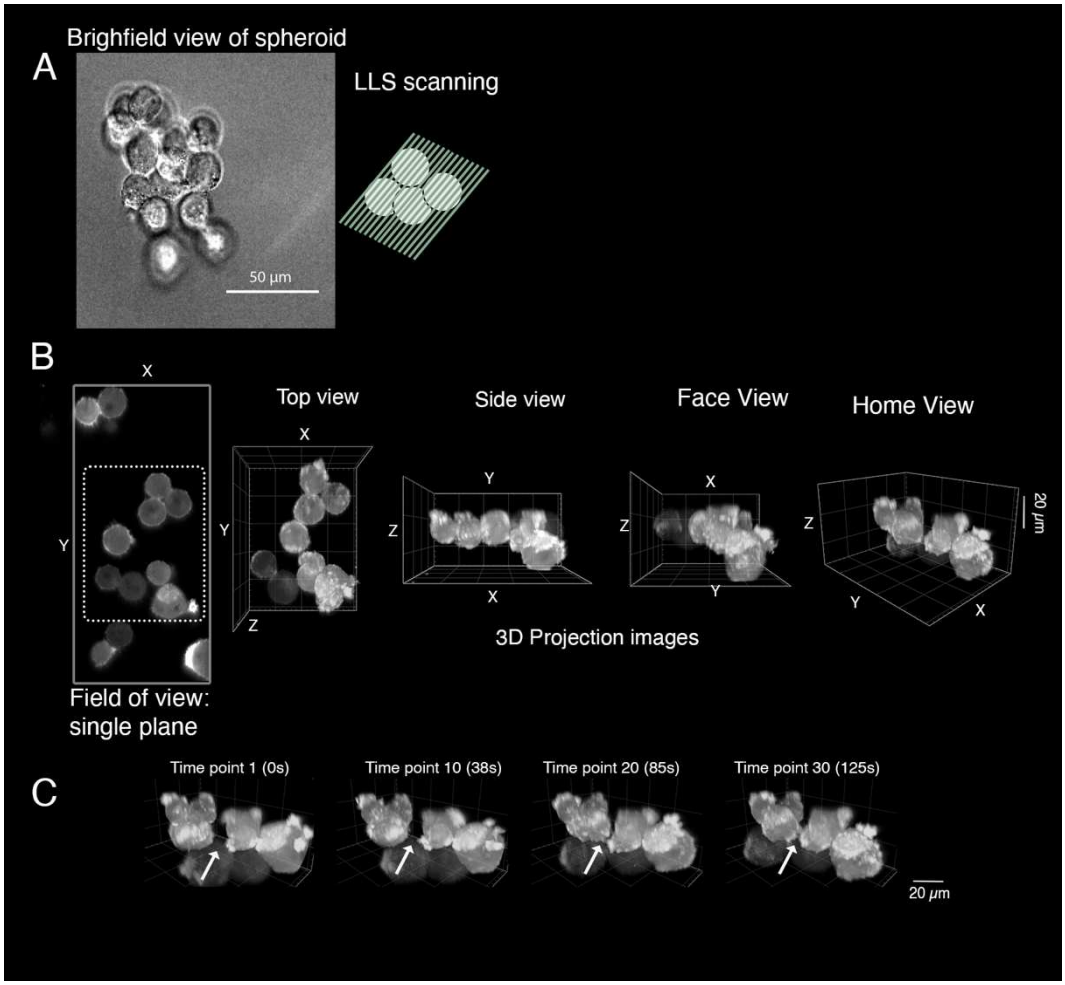

Figure 5: Lattice light sheet imaging of a small spheroid (cells express eGFP-Lifeact). A: shows a brightfield image of a spheroid. The adjacent diagram shows how the light sheet (green lines) is scanned across the spheroid. For the example shown in B and C, 380 slices in the Z direction were obtained (54.95 µm) per time point, X was 14.83 µm, Y was 317.82 µm. and each scan took ~4s. The image was then deskewed to generate the final images. B: shows a single plane of the resulting deskewed image (for eGFP-Lifeact expressing cells), and 3D projection images viewing the spheroid from different angles. (Top, side and face and home views). C. shows the side view at different time points: the arrow shows how two cells move together and interact within the spheroid.

References

Allen, J. R., Ross, S. T. and Davidson, M. W. (2013). Sample preparation for single molecule localization microscopy. *Phys Chem Chem Phys* **15**, 18771-83.

Betzig, E., Patterson, G. H., Sougrat, R., Lindwasser, O. W., Olenych, S., Bonifacino, J. S., Davidson, M. W., Lippincott-Schwartz, J. and Hess, H. F. (2006). Imaging intracellular fluorescent proteins at nanometer resolution. *Science* **313**, 1642-5.

Bukhari, H. and Muller, T. (2019). Endogenous Fluorescence Tagging by CRISPR. *Trends Cell Biol* **29**, 912-928.

Chalfie, M., Tu, Y., Euskirchen, G., Ward, W. W. and Prasher, D. C. (1994). Green fluorescent protein as a marker for gene expression. *Science* **263**, 802-5.

Chen, B. C., Legant, W. R., Wang, K., Shao, L., Milkie, D. E., Davidson, M. W., Janetopoulos, C., Wu, X. S., Hammer, J. A., 3rd, Liu, Z. et al. (2014). Lattice light-sheet microscopy: imaging molecules to embryos at high spatiotemporal resolution. *Science* **346**, 1257998.

Cranfill, P. J., Sell, B. R., Baird, M. A., Allen, J. R., Lavagnino, Z., de Gruiter, H. M., Kremers, G. J., Davidson, M. W., Ustione, A. and Piston, D. W. (2016). Quantitative assessment of fluorescent proteins. *Nat Methods* **13**, 557-62.

Curd, A., Cleasby, A., Makowska, K., York, A., Shroff, H. and Peckham, M. (2015). Construction of an instant structured illumination microscope. *Methods* **88**, 37-47.

Curd, A. P., Leng, J., Hughes, R. E., Cleasby, A. J., Rogers, B., Trinh, C. H., Baird, M. A., Takagi, Y., Tiede, C., Sieben, C. et al. (2021). Nanoscale Pattern Extraction from Relative Positions of Sparse 3D Localizations. *Nano Lett* **21**, 1213-1220.

Dabiri, G. A., Turnacioglu, K. K., Sanger, J. M. and Sanger, J. W. (1997). Myofibrillogenesis visualized in living embryonic cardiomyocytes. *Proc Natl Acad Sci U S A* **94**, 9493-8.

Dempsey, G. T., Vaughan, J. C., Chen, K. H., Bates, M. and Zhuang, X. (2011). Evaluation of fluorophores for optimal performance in localization-based super-resolution imaging. *Nat Methods* **8**, 1027-36.

Dunn, S., Morrison, E. E., Liverpool, T. B., Molina-Paris, C., Cross, R. A., Alonso, M. C. and Peckham, M. (2008). Differential trafficking of Kif5c on tyrosinated and detyrosinated microtubules in live cells. *J Cell Sci* **121**, 1085-95.

Guo, M., Li, Y., Su, Y., Lambert, T., Nogare, D. D., Moyle, M. W., Duncan, L. H., Ikegami, R., Santella, A., Rey-Suarez, I. et al. (2020). Rapid image deconvolution and multiview fusion for optical microscopy. *Nat Biotechnol* **38**, 1337-1346.

Gustafsson, M. G. (2000). Surpassing the lateral resolution limit by a factor of two using structured illumination microscopy. *J Microsc* **198**, 82-7.

Haywood, N. J., Wolny, M., Rogers, B., Trinh, C. H., Shuping, Y., Edwards, T. A. and Peckham, M. (2016). Hypertrophic cardiomyopathy mutations in the calponin-homology domain of ACTN2 affect actin binding and cardiomyocyte Z-disc incorporation. *Biochem J* **473**, 2485-93.

Heilemann, M., van de Linde, S., Mukherjee, A. and Sauer, M. (2009). Super-resolution imaging with small organic fluorophores. *Angew Chem Int Ed Engl* **48**, 6903-8.

Heilemann, M., van de Linde, S., Schuttpelz, M., Kasper, R., Seefeldt, B., Mukherjee, A., Tinnefeld, P. and Sauer, M. (2008). Subdiffraction-resolution fluorescence imaging with conventional fluorescent probes. *Angew Chem Int Ed Engl* **47**, 6172-6.

Hell, S. W. and Wichmann, J. (1994). Breaking the diffraction resolution limit by stimulated emission: stimulated-emission-depletion fluorescence microscopy. *Opt Lett* **19**, 780-2.

Hess, S. T., Girirajan, T. P. and Mason, M. D. (2006). Ultra-high resolution imaging by fluorescence photoactivation localization microscopy. *Biophys J* **91**, 4258-72.

Hobson, C. M., Aaron, J. S., Heddleston, J. M. and Chew, T. L. (2021). Visualizing the Invisible: Advanced Optical Microscopy as a Tool to Measure Biomechanical Forces. *Front Cell Dev Biol* **9**, 706126.

Huisken, J., Swoger, J., Del Bene, F., Wittbrodt, J. and Stelzer, E. H. (2004). Optical sectioning deep inside live embryos by selective plane illumination microscopy. *Science* **305**, 1007-9.

Jacquemet, G., Carisey, A. F., Hamidi, H., Henriques, R. and Leterrier, C. (2020). The cell biologist's guide to super-resolution microscopy. *J Cell Sci* **133**.

Ketchen, S., Rohwedder, A., Knipp, S., Esteves, F., Struve, N., Peckham, M., Ladbury, J. E., Curd, A., Short, S. C. and Bruning-Richardson, A. (2020). A novel workflow for three-dimensional analysis of tumour cell migration. *Interface Focus* **10**, 20190070.

Klar, T. A. and Hell, S. W. (1999). Subdiffraction resolution in far-field fluorescence microscopy. *Opt Lett* **24**, 954-6.

Lambert, T. J. (2019). FPbase: a community-editable fluorescent protein database. *Nat Methods* **16**, 277-278.

Liu, J. and Cui, Z. (2020). Fluorescent Labeling of Proteins of Interest in Live Cells: Beyond Fluorescent Proteins. *Bioconjug Chem* **31**, 1587-1595.

Lopata, A., Hughes, R., Tiede, C., Heissler, S. M., Sellers, J. R., Knight, P. J., Tomlinson, D. and Peckham, M. (2018). Affimer proteins for F-actin: novel affinity reagents that label F-actin in live and fixed cells. *Sci Rep* **8**, 6572.

Lukinavicius, G., Reymond, L., D'Este, E., Masharina, A., Gottfert, F., Ta, H., Guther, A., Fournier, M., Rizzo, S., Waldmann, H. et al. (2014). Fluorogenic probes for live-cell imaging of the cytoskeleton. *Nat Methods* **11**, 731-3.

Makowska, K. A., Hughes, R. E., White, K. J., Wells, C. M. and Peckham, M. (2015). Specific Myosins Control Actin Organization, Cell Morphology, and Migration in Prostate Cancer Cells. *Cell Rep* **13**, 2118-25.

Manley, S., Gillette, J. M., Patterson, G. H., Shroff, H., Hess, H. F., Betzig, E. and Lippincott-Schwartz, J. (2008). High-density mapping of single-molecule trajectories with photoactivated localization microscopy. *Nat Methods* **5**, 155-7.

McKinney, S. A., Murphy, C. S., Hazelwood, K. L., Davidson, M. W. and Looger, L. L. (2009). A bright and photostable photoconvertible fluorescent protein. *Nat Methods* **6**, 131-3.

Ponjavic, A., McColl, J., Carr, A. R., Santos, A. M., Kulenkampff, K., Lippert, A., Davis, S. J., Klenerman, D. and Lee, S. F. (2018). Single-Molecule Light-Sheet Imaging of Suspended T Cells. *Biophys J* **114**, 2200-2211.

Remenyi, R., Gao, Y., Hughes, R. E., Curd, A., Zothner, C., Peckham, M., Merits, A. and Harris, M. (2018). Persistent Replication of a Chikungunya Virus Replicon in Human Cells Is Associated with Presence of Stable Cytoplasmic Granules Containing Nonstructural Protein 3. *J Virol* **92**.

Riedl, J., Crevenna, A. H., Kessenbrock, K., Yu, J. H., Neukirchen, D., Bista, M., Bradke, F., Jenne, D., Holak, T. A., Werb, Z. et al. (2008). Lifeact: a versatile marker to visualize F-actin. *Nat Methods* **5**, 605-7.

Rust, M. J., Bates, M. and Zhuang, X. (2006). Sub-diffraction-limit imaging by stochastic optical reconstruction microscopy (STORM). *Nat Methods* **3**, 793-5.

Schermelleh, L., Ferrand, A., Huser, T., Eggeling, C., Sauer, M., Biehlmaier, O. and Drummen, G. P. C. (2019). Super-resolution microscopy demystified. *Nat Cell Biol* **21**, 72-84.

Schindelin, J., Arganda-Carreras, I., Frise, E., Kaynig, V., Longair, M., Pietzsch, T., Preibisch, S., Rueden, C., Saalfeld, S., Schmid, B. et al. (2012). Fiji: an open-source platform for biological-image analysis. *Nat Methods* **9**, 676-82.

Stirling, D. R., Swain-Bowden, M. J., Lucas, A. M., Carpenter, A. E., Cimini, B. A. and Goodman, A. (2021). CellProfiler 4: improvements in speed, utility and usability. *BMC Bioinformatics* **22**, 433.

Stringer, C., Wang, T., Michaelos, M. and Pachitariu, M. (2021). Cellpose: a generalist algorithm for cellular segmentation. *Nat Methods* **18**, 100-106.

Swailes, N. T., Colegrave, M., Knight, P. J. and Peckham, M. (2006). Non-muscle myosins 2A and 2B drive changes in cell morphology that occur as myoblasts align and fuse. *J Cell Sci* **119**, 3561-70.

Swailes, N. T., Knight, P. J. and Peckham, M. (2004). Actin filament organization in aligned prefusion myoblasts. *J Anat* **205**, 381-91.

Wiedenmann, J., Ivanchenko, S., Oswald, F., Schmitt, F., Rocker, C., Salih, A., Spindler, K. D. and Nienhaus, G. U. (2004). EosFP, a fluorescent marker protein with UV-inducible green-to-red fluorescence conversion. *Proc Natl Acad Sci U S A* **101**, 15905-10.

Wilson, T. (2011). Resolution and optical sectioning in the confocal microscope. *J Microsc* **244**, 113-21.

Yang, T. T., Cheng, L. and Kain, S. R. (1996). Optimized codon usage and chromophore mutations provide enhanced sensitivity with the green fluorescent protein. *Nucleic Acids Res* **24**, 4592-3.

York, A. G., Chandris, P., Nogare, D. D., Head, J., Wawrzusin, P., Fischer, R. S., Chitnis, A. and Shroff, H. (2013). Instant super-resolution imaging in live cells and embryos via analog image processing. *Nat Methods* **10**, 1122-6.

Zhang, M., Chang, H., Zhang, Y., Yu, J., Wu, L., Ji, W., Chen, J., Liu, B., Lu, J., Liu, Y. et al. (2012). Rational design of true monomeric and bright photoactivatable fluorescent proteins. *Nat Methods* **9**, 727-9.

Further Reading

Useful Reviews;

Grimm, J. B. and Lavis, L. D. (2022). Caveat fluorophore: an insiders' guide to small-molecule fluorescent labels. *Nat Methods* **19**, 149-158. (Hobson et al., 2021)
Jacquemet, G., Carisey, A. F., Hamidi, H., Henriques, R. and Leterrier, C. (2020). The cell biologist's guide to super-resolution microscopy. *J Cell Sci* **133**.**Lemon, W. C. and McDole, K.** (2020). Live-cell imaging in the era of too many microscopes. *Curr Opin Cell Biol* **66**, 34-42.
Reiche, M. A., Aaron, J. S., Boehm, U., DeSantis, M. C., Hobson, C. M., Khuon, S., Lee, R. M. and Chew, T. L. (2022). When light meets biology - how the specimen affects quantitative microscopy. *J Cell Sci* **135**.
Schermelleh, L., Ferrand, A., Huser, T., Eggeling, C., Sauer, M., Biehlmaier, O. and Drummen, G. P. C. (2019). Super-resolution microscopy demystified. *Nat Cell Biol* **21**, 72-84.

Online microscopy Resources, https://www.rms.org.uk/library/online-microscopy-resources.html
And courses and workshops run by the Royal Microscopical Society:
https://www.rms.org.uk/

Nikon Microscopy: https://www.microscopyu.com/
For many useful articles on imaging, explaining the basics.

https://myscope.training/
on-line training in microscopy